Chaos

Interactions of solitary waves in integrable and nonintegrable lattices

Cite as: Chaos **30**, 043101 (2020); https://doi.org/10.1063/1.5121427
Submitted: 24 July 2019 . Accepted: 10 March 2020 . Published Online: 01 April 2020

Guo Deng, Gino Biondini, and Surajit Sen

Chaos ARTICLE scitation.org/journal/cha

Interactions of solitary waves in integrable and nonintegrable lattices

Cite as: Chaos 30, 043101 (2020); doi: 10.1063/1.5121427
Submitted: 24 July 2019 · Accepted: 10 March 2020 ·
Published Online: 1 April 2020

Guo Deng,[1,2,a)] Gino Biondini,[1,3,b)] and Surajit Sen[1,c)]

AFFILIATIONS

[1] Department of Physics, The State University of New York at Buffalo, Buffalo, New York 14260, USA
[2] Department of Mathematics and Statistics, Macquarie University, Sydney, New South Wales 2109, Australia
[3] Department of Mathematics, The State University of New York at Buffalo, Buffalo, New York 14260, USA

[a)] **Electronic mail:** guodeng@buffalo.edu
[b)] **Electronic mail:** biondini@buffalo.edu
[c)] **Author to whom correspondence should be addressed:** sen@buffalo.edu

ABSTRACT

We study how the dynamics of solitary wave (SW) interactions in integrable systems is different from that in nonintegrable systems in the context of crossing of two identical SWs in the (integrable) Toda and the (non-integrable) Hertz systems. We show that the collision process in the Toda system is perfectly symmetric about the collision point, whereas in the Hertz system, the collision process involves more complex dynamics. The symmetry in the Toda system forbids the formation of secondary SWs (SSWs), while the absence of symmetry in the Hertz system allows the generation of SSWs. We next show why the experimentally observed by-products of SW–SW interactions, the SSWs, must form in the Hertz system. We present quantitative estimations of the amount of energy that transfers from the SW after collision to the SSWs using (i) dynamical simulations, (ii) a phenomenological approach using energy and momentum conservation, and (iii) using an analytical solution introduced earlier to describe the SW in the Hertz system. We show that all three approaches lead to reliable estimations of the energy in the SSWs.

Solitary wave–solitary wave interactions in non-integrable systems are highly non-trivial compared to those in integrable systems. In non-integrable systems, the energies of two interacting solitary waves are reduced after the interaction. There has been a limited number of studies that address the interaction between solitary waves in non-integrable systems. Among non-integrable systems, the Hertz chain is of particular interest because it models an experimentally realizable physical system. Solitary wave–solitary wave interactions in Hertz systems have been studied via dynamical simulations and laboratory experiments. Results show that secondary solitary waves carrying a small fraction of the energy of the original solitary wave form post-interaction. The precise magnitude of energy carried by the secondary waves is known to depend on the softness of the boundaries where the secondary waves form. Formation of secondary solitary waves in turn lead to the reduction of the energy of the scattered solitary waves. However, questions such as why the secondary solitary waves must form and whether one can obtain a quantitative characterization of the energy of the secondary solitary waves have remained largely unresolved. In this work, we use a phenomenological approach, an analytical approach based on the analytical solution to the solitary wave by Sen and Manciu, and dynamical simulations to calculate the energy reduction of the solitary waves and hence infer the total energy used in the generation of one or more secondary solitary waves that form after the solitary wave–solitary wave interaction.

I. INTRODUCTION

Solitary waves (SWs), which are just about ubiquitous in nonlinear systems, have been studied extensively. Among the nonlinear systems admitting SWs, a special class known as integrable systems has been an active research topic for decades because of their rich mathematical structures and physical applications.[1] However, many nonlinear systems encountered in nature that admit SW solutions are non-integrable. Therefore, it is important to study the similarities and differences between integrable and non-integrable systems.

The key difference between integrable systems and non-integrable systems is reflected in the interactions between SWs. In the integrable and non-integrable systems, the interaction induces phase or position shifts of the SWs, which are due to the waves traveling through one another.[2,3] It may be noted that interactions between SWs leading to the production of lower energy SWs post collision were first reported in a numerical study for another non-integrable system, the Fermi–Pasta–Ulam–Tsingou system,[4] by Flytzanis *et al.* and more recently for the same system by Zhao *et al.*[5,6] Naturally, the production of low energy SWs post collision means the colliding SWs are left with lower energy post collision. Hence, understanding the differences between integrable and non-integrable systems hinges upon understanding the underlying reasons for the reduction in the SW energy after collision in the non-integrable systems.

In this paper, we focus on SW interactions in discrete integrable and non-integrable systems. Specifically, we consider a one-dimensional lattice with nearest neighbor interactions. The lattice is described by a system of differential-difference equations as follows:

$$m\frac{d^2y_n}{dt^2} = \phi'(y_{n+1} - y_n) - \phi'(y_n - y_{n-1}), \tag{1}$$

where m denotes the particle mass, y_n denotes the displacement of the nth particle with respect to its equilibrium, ϕ denotes the interaction potential, and ϕ' denotes the space derivative of ϕ.

In general, (1) is nonlinear and cannot be treated analytically. However, for integrable lattices, one can use mathematical tools such as the inverse scattering transform to obtain explicit solutions.[1] A typical example of integrable lattices is the celebrated Toda lattice,[7–10] which has an interaction potential given by

$$\phi(r_n) = \frac{a}{b}\,\mathrm{e}^{-br_n} + ar_n, \quad a, b \in \text{constants}, \tag{2}$$

with $r_n = y_{n+1} - y_n$ being the mutual displacement. The Toda system has attracted a significant amount of research over the decades.[11–14]

Among numerous nonintegrable systems, the Hertz chain[15–20] is of particular interest. It serves as a model to describe the repelling force that comes into play when the contact area between two adjacent elastic or granular spheres increases, the so-called Hertz force.[21] The Hertz interaction potential is given by

$$\phi(r_n) = \begin{cases} c|r_n|^{5/2}, & r_n \le 0, \\ 0, & r_n > 0, \end{cases} \quad c \in \text{constant}, \tag{3}$$

where $c = (2/[5D(Y,\sigma)])(R/2)^{1/2}$, R is the radius of the particle, $D(Y,\sigma) = (3/2)[(1-\sigma^2)/Y]$, and Y and σ denote Young's modulus and Poisson's ratio, respectively. Note that the Hertz potential goes to zero when the compression goes to zero and cannot take on negative values.

In the Toda lattice, SWs maintain their amplitude and velocity after they interact with each other,[7,10] while in the Hertz chain, SW interactions induce formation of so-called secondary solitary waves (SSWs), which carry a small amount of energy compared to the original SWs and was first suggested on the basis of dynamical simulations in Refs. 22–25. At this stage, it may be useful to mention two important issues. First, we emphasize that the SSWs do not appear in our studies somehow due to a numerical error. As discussed in detail in Fig. 4 of Ref. 22, the numerical error due to simulations is 9 orders of magnitude smaller in energy than the energy carried by the SSWs. Furthermore, the existence of the SSWs was experimentally confirmed in Fig. 3 of Ref. 25. In Figs. 3(b) and 3(c) of Ref. 25, the authors showed that for their specific system, the SSWs obtained via simulations for SW collisions with soft end walls and seen in experiments were in good agreement. The simulations, however, ignored dissipation, and any lack of agreement between the simulations and the experiments was attributed to the challenges associated with correctly accounting for dissipation. Second, when the colliding SWs have the same energy and they collide either at a grain center[25] or in a grain edge,[3] we call them symmetric collisions. In Ref. 25, the authors examined the grain-center collision problem approximately by replacing the system by a half chain with a hard end wall. However, no end wall is infinitely hard, and this led to the probing of the effects of wall softness, which slows down the SW-wall collision process and in turn leads to SSWs that carry more energy than in the hard wall limit. This issue was later examined via simulations.[26] It should be noted that SSWs produced from SW–SW collisions in chains carry very small amounts of energy, and these SSWs remain to be experimentally identified.

These SSWs describe the nature of interactions between the SWs. Hence, a detailed understanding of SSWs is needed to understand how these strongly nonlinear and non-integrable systems behave when held between boundaries as time evolves and eventually approach the so-called quasi-equilibrium state[26–30] and at even later times, the equilibrium state.[31] In the context of purely granular systems, one may wonder as to why suggestions of the existence of quasi-equilibrium and the possible transition of the same to equilibrium are relevant because it would be very difficult to see quasi-equilibrium in a granular chain due to inherent effects of dissipation. Notwithstanding this argument, we contend that the concept itself may have broader applicability. For example, in nonlinear chains, such as those of quantum spins in optical lattices in 1D and in 3D nonlinear systems such as in carbon nanotubes, evidence of quasi-equilibrium (similar concepts have been suggested with names such as quasithermal or prethermal) behavior may indeed have been seen already.[32,33]

However, questions such as why the SSWs do not form in the Toda lattice but must form in the Hertz chain and whether one can obtain a quantitative characterization of the SSWs remain open issues. This paper is devoted to address why SSWs form in non-integrable systems during grain-center collisions. We discuss in detail below the nature of the SW–SW collision and show how the central grain remains at rest at all times in the Hertz and Toda systems, while the grains in the immediate neighborhood of the center move differently in the two systems.

The structure of this paper is as follows: in Sec. II, we study crossing of identical SWs in Toda and Hertz systems; in Sec. III, we investigate the relation between energy and momentum of a SW; in Sec. IV, we show why SSWs must form in the Hertz system as well as an estimation of the amount of energy that ends up being used to produce the SSWs; and in Sec. V, we investigate whether the solution proposed by Sen and Manciu in the Hertz chain obtained in Refs. 34 and 35 can capture the main features of SSWs. The work ends with a summary in Sec. VI.

II. CROSSING OF IDENTICAL SOLITARY WAVES IN TODA AND HERTZ SYSTEMS

We consider finite lattices with $N = 201$ particles. Open boundary conditions are used at the two ends of the system in order to avoid effects of collisions between the edge grains and the walls. For the Hertz system, we use numbers that allow for convenient energies of the SSWs. Specifically, we take $D = 5.0 \times 10^{-8}\,\mathrm{m}^2/\mathrm{N}$, $R = 0.05\,\mathrm{m}$, and $m = 1.0\,\mathrm{kg}$, and we use the velocity Verlet algorithm, which is time tested and a symplectic integrator,[36] with time step $dt = 1.0 \times 10^{-9}\,\mathrm{s}$ and a total step $N_{\mathrm{step}} = 3 \times 10^7$; the maximum difference of total energy across the length of our runs is at the order of 10^{-11} J. In our discussion, the Toda system is nondimensional, and the units used in the Hertz system are SI units. The velocity Verlet algorithm is predictor–corrector and returns the position and the velocity to the same order of accuracy. It is also a fast and time tested algorithm, which has been widely used in Molecular Dynamics simulations for decades.[36]

SWs with the same amplitude but opposite velocity are generated via simultaneous velocity impulses with the same magnitude but opposite direction at both ends of the chain. The behavior of the kinetic energy (KE) of two SWs as a function of time is shown in Figs. 1(a) and 1(b) for both systems.

The oscillating region at the top of Figs. 1(a) and 1(b) represents the zone where two SWs are well separated from each other.

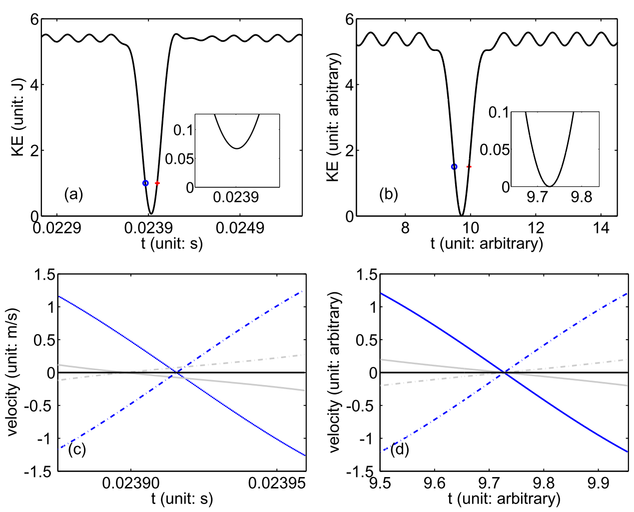

FIG. 1. The KE of two solitary waves as a function of time in Hertz (a) and Toda (b) systems. The red (left side) and blue (right side) dots represent instants at which the system has the same KE. The velocity of the 103rd (dashed gray line), 102nd (dashed blue line), 100th (solid blue line), and 99th particle (solid gray line) as a function of time in the collision process in the Hertz (c) and Toda (d) systems. The solid black line represents the 101st or the central particle in the system in (c) and (d).

The central dip represents the region where SWs come across and interact with each other; at that point, the system gets compressed and the KE converts to the potential energy (PE).

A significant difference between the two systems is that, for the Toda system, by decreasing the time step, the $\mathrm{KE}_{\mathrm{min}}$ approaches 0; whereas in the Hertz system, $\mathrm{KE}_{\mathrm{min}}$ never approaches 0. The difference suggests that in the Toda system, all particles stop simultaneously, while this synchronization is absent in the Hertz system. Another difference is that the KE is asymmetric about its minimum in Fig. 1(a), whereas it is perfectly symmetric about the minimum in Fig. 1(b). In addition, we find that the velocities of the 99th and 100th particles as a function of time in the collision process are given in Figs. 1(c) and 1(d). The dynamics of the 102nd and 103rd particles are opposite in velocity vs time compared to the 100th and 99th particles. The 101st particle, which is at the center, does not move at all during the entire process of collision in both cases and is described by the solid black horizontal line in Figs. 1(c) and 1(d). As one can see, in the Hertz system, different particles switch directions at different instants.

Recall that the two-soliton solution in the Toda system is given by

$$y_n = \log(1 + A_1\,\mathrm{e}^{2(\kappa_1 n-\beta_1 t)} + A_2\,\mathrm{e}^{2(\kappa_2 n-\beta_2 t)} + \mathrm{e}^{2[(\kappa_1+\kappa_2)n-(\beta_1+\beta_2)t+\delta]}), \tag{4}$$

where

$$\beta_1^2 = \sinh^2\kappa_1, \quad \beta_2^2 = \sinh^2\kappa_2,$$
$$\delta = \frac{1}{2}\log\left(\frac{\sinh^2(\kappa_1-\kappa_2) - (\beta_1-\beta_2)^2}{A_1A_2[(\beta_1+\beta_2)^2 - \sinh^2(\kappa_1+\kappa_2)]}\right), \tag{5}$$

and for simplicity, we set the parameters a, b, and m equal to 1. For the two-soliton solution, we have four independent parameters: κ_1, κ_2, A_1, and A_2.

For two SWs with the same amplitude but opposite velocity, $\kappa_1 = \kappa_2$ and $\beta_1 = -\beta_2$. We can show that at $t_0 = [1/(4\beta_1)]\log(A_1/A_2)$, the velocity profile

$$v(n, t_0) = 0 \quad \forall n. \tag{6}$$

Moreover, the motion of two SWs is symmetric about $t = t_0$, i.e., for t_1 and t_2 such that $(t_1 + t_2)/2 = t_0$, we have

$$y(n, t_1) = y(n, t_2), \quad v(n, t_1) = -v(n, t_2). \tag{7}$$

From the analysis above, we can see that crossing of identical SWs in the Toda system is perfectly symmetric about the instant when every particle stops simultaneously; the motion after that instant is simply the reverse of the motion before that instant.

For comparison purposes, Fig. 2 shows velocity profiles at instants denoted in Fig. 1 from numerics in the Toda and Hertz systems. For the Toda system, the velocity profiles are opposite, while for the Hertz system, the velocity profiles are not opposite; i.e., the velocity profile after collision cannot be obtained by simply reversing the velocity profile before collision.

If we imagine that our SW in the Toda lattice is bouncing off a wall instead of two of them crossing, it is easy to see that the SW behaves as a rather rigid object for it to bounce off intact. In the Hertz system, the grains turn around at distinct times as is evident

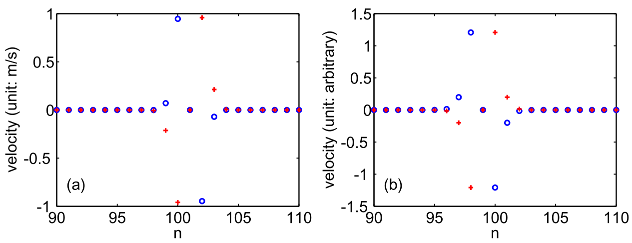

FIG. 2. Figures (a) and (b) represent velocity profiles in the Hertz and Toda systems at instants denoted in Fig. 1, respectively. Note that circles represent the instant before KE_{min}, while crosses represent the instant after KE_{min}.

from Fig. 1(c). This behavior is in sharp contrast to how the particles turn around simultaneously as shown in Fig. 1(d). We suggest that the key difference between non-integrable and integrable systems may lie in how the SW turnaround process occurs, with turn around at a unique time being the case for integrable systems and at different times being the case for non-integrable systems. Our future studies will test this suggested way of recognizing an integrable vs a non-integrable SW bearing system.

III. THE ENERGY AND MOMENTUM OF A SW

For both Toda and Hertz systems, as a SW propagates along the lattice, both the KE and PE oscillate but add up to a constant. Other than the total energy, the momentum of a SW is a constant. It is, therefore, relevant to investigate the relation between these conserved quantities.

For the Toda system, thanks to the explicit one-soliton solution, we can obtain how the total energy and momentum of a SW depend on the soliton parameter κ,[7–10]

$$p_{SW} = \sinh\kappa, \tag{8a}$$

$$E_{SW} = 2(\sinh\kappa\cosh\kappa - \kappa). \tag{8b}$$

Therefore, the energy–momentum curve can be obtained as a parameterized curve in the left panel of Fig. 3.

For the Hertz system, we do not have exact an one-soliton solution; therefore, we measured total energy and momentum of the SW numerically, and we plotted the numerical data on a log–log plot. The data suggest that the relation between total energy and momentum is given by

$$E_{SW} = cp_{SW}^2, \tag{9}$$

where $c = 0.383\,433$, and it depends on the system parameters chosen for the simulation.

The notion of the SW as a quasiparticle with its total energy depending quadratically on its momentum was first reported by Tichler *et al.* [see Eq. (2) in Ref. 37] and helps us develop a phenomenological model to quantitatively characterize SWs and study the formation of SSWs during SW–SW collision in the Hertz system.

We further note that the energy–momentum curve in these systems are monotonic functions.

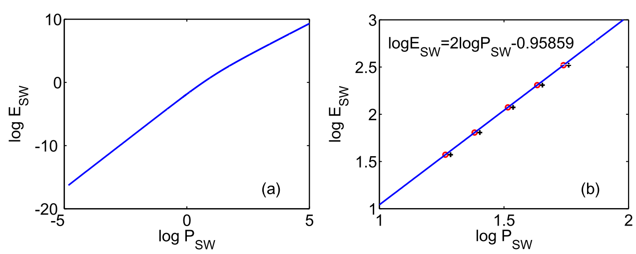

FIG. 3. The energy–momentum curve of a SW in Toda (a) and Hertz (b) systems. In Fig. (b), the discrete dots are from numerics and the line is the fitting function. The black crosses represent energy and momentum of the reflected bundles right after collision, and the corresponding incident SWs are given by the adjacent dots.

IV. SECONDARY SW FORMATION IN THE HERTZ SYSTEM: A REVISIT

In this section, we examine why SSWs must form in the Hertz system. A quantitative characterization of the SSWs in the Hertz system is developed by making use of the energy–momentum relation discussed in Sec. III.

In considering the collision of two SWs, we observe that while the total momentum of the system is conserved, due to the presence of effective forces in the wall that mimics the collision point, the total momentum of the half system is not conserved. Recall in the collision process, the 101st particle suffers no motion (see Fig. 1), and the motion on both sides of the 101st particle is symmetric to each other.

The change in the total momentum of the 1st to 100th particle is directly related to the interaction force in the contact surface between the 100th and 101st particles, and a plot of this force as a function of time is given in Fig. 4. During the time interval $(0, t_1)$ (marked by the first dot in Fig. 4), the force between the 100th and 101st particles is zero; as a result, the total momentum of the half system is conserved for this part of the motion. During the time interval (t_1, t_2) (marked by the second dot in Fig. 4), the 100th particle compresses the 101st particle and then decompresses from the same, and

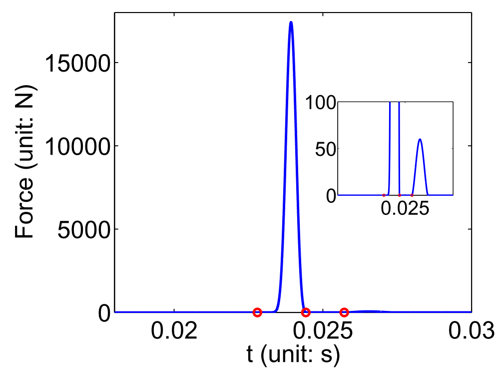

FIG. 4. The interaction force in the contact surface between the 100th and 101st particles as a function of time. The three dots denote instants t_1, t_2, and t_3, respectively. The inset shows the same data as the main figure but with much higher resolution so that the recoil of the 100th particle can be seen.

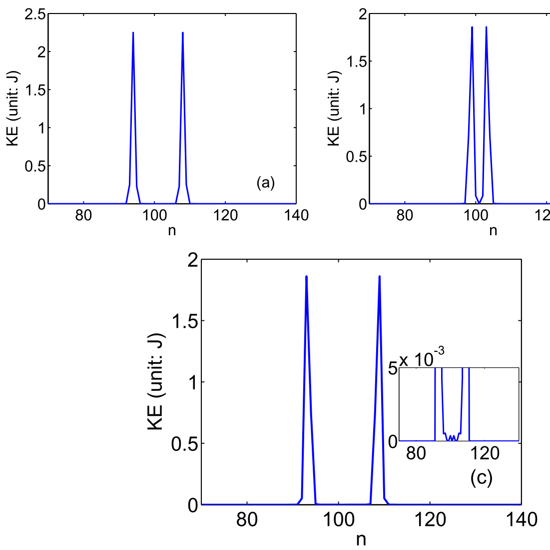

FIG. 5. The kinetic energy of the grains is shown at the times denoted by dots in Fig. 4. Here, (a) describes the SWs as they are about to collide, (b) just when the post-collision SWs emerge, and (c) after the first few SSWs have formed, which are not visible in the scale used in the main figure but can be clearly seen under higher energy resolution in the inset.

consequently, the momentum of the half system switches direction during this time period. During the time interval (t_2, t_3) (marked by the third dot in Fig. 4), the force is at a plateau, until the 100th particle recoils at $t = t_3$. At this plateau, the force is of the order of 10^{-6} N; consequently, the momentum of the half system is conserved up to 10^{-11} N s.

We plot the KE vs position at $t = t_1, t_2$, and t_3, respectively. Figure 5(a) shows two energy bundles at $t = t_1$ before collision, Fig. 5(b) shows that two reflected energy bundles are formed at $t = t_2$ right after the collision, and Fig. 5(c) shows that at $t = t_3$, the reflected energy bundles split into the leading pulses and trailing pulses.

We measured the magnitude of the momentum of the newly formed reflected energy bundle immediately after the interaction in Fig. 5(b). This magnitude turns out to be *different* from the magnitude of the momentum of the incident SW in Fig. 5(a). Note that by energy conservation, the bundles in Fig. 5(b) hold the same amount of energy as the incident SWs in Fig. 5(a). If we put reflected bundles in Fig. 5(b) in the energy–momentum plot, they correspond to the black dots in Fig. 3(b), which does not fall on the energy–momentum line. Therefore, it is impossible to describe the energy bundle in Fig. 5(b) as one SW. Observe that the Hertz system without precompression can only make SWs as stable energy carriers. Hence, the reflected bundle results in the formation of what seems like a train of SWs. Earlier work[23] has shown that these reflected SWs do not quite make a train because SSW energies can vary significantly regardless of when they are born as a function of time. The black dots in Fig. 3(b) lie very close to the energy–momentum line of a SW; one, therefore, expect the leading

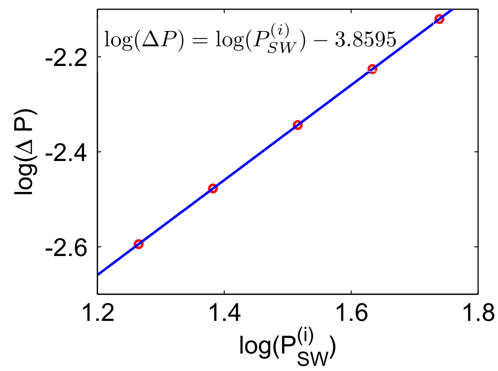

FIG. 6. The change in momentum of the reflected energy bundle shown in Fig. 5(b) with respect to the momentum of incident SW shown in Fig. 5(a) as a function of the incident momentum.

SW after collision carries the majority of the energy, while the SWs following behind carry only a small amount of the energy.[22–24] Due to the smallness in energy, the subsequent SWs are termed "SSWs."

The formation of SSWs is a highly nontrivial process that is not well understood at the theoretical level.[23,24] The time scale of such a process is far beyond the time interval (t_2, t_3). However, we note that during the time interval (t_2, t_3), the leading SWs post collision are formed. If we can obtain the energy of the leading reflected SWs after collision, we can attempt to learn about the total energy used to generate the SSWs by taking the difference between the leading SWs before and after collision. Simulations[23,24] clearly show that many more SSWs form as time progresses, which carry very small amounts of energy compared to the first SSW. It is important to note that the magnitude of SSWs is such that they may not be regarded as a solitary wave train.[23] As one can see right after time $t = t_3$, the 100th particle recoils, which brings further momentum change to the half chain and, therefore, induces the generation of more SSWs. Since our model is focused on the time interval (t_1, t_3) and our main goal is to obtain the energy carried by the leading reflected pulse, it is reasonable for us to bind all the SSWs as one SSW. We denote these post-collision SWs with the superscript (r) below.

First, it is easy to see that energy is conserved in this collision. By equating the energy of the incident SW, $E^{(i)}_{SW}$, at $t = t_1$ to the

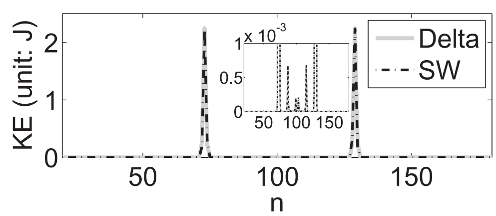

FIG. 7. A comparison between SSWs generated by opposite delta velocity impulses (solid gray line) and those by the analytical SW solution of Sen and Manciu in Eq. (12) (black dotted line).[34]

TABLE I. Comparison of the energy devoted to generate SSWs between our phenomenological model and numerical simulations with the initial condition given by opposite delta velocity impulses is shown. To test the effectiveness of the analytical SW solution for the Hertz chain in Sec. V (12), we also compare energy of SSWs generated by (12) and that generated by opposite delta velocity impulses. The units in the table are SI units. We find that the analytical solution yields a result that is closest to that obtained with the dynamical simulations, while the result based on applying energy and momentum conservation is less accurate (see discussion above).

$P_{incident}$	$E_{SSW,\,dyn}$	$E_{SSW,\,phenom}$	Percent error	$E_{SSW,\,theo}$	Percent error
3.5434	0.002 150 0	0.002 200 8	2.3644	0.002 193 1	2.0069
3.9841	0.002 718 0	0.002 782 2	2.3632	0.002 837 9	2.0032
4.5532	0.003 550 0	0.003 633 9	2.3644	0.003 706 7	2.0028
5.1224	0.004 493 0	0.004 599 2	2.3637	0.004 691 4	2.0045
5.6915	0.005 546 9	0.005 678 0	2.3639	0.005 791 8	2.0048

energy at t_3, which is a summation of $\mathrm{E}_{SW}^{(r)}$ and $\mathrm{E}_{SSW}^{(r)}$, we obtain the equation for energy conservation.

Let us then investigate the momentum of the system. We find that during the time interval (t_2,t_3), the total momentum of the half chain is conserved to 10^{-11} N s. Thus, let us say that the momentum carried by the reflected bundle in Fig. 5(b) at t_2 must equal the sum of $|\mathrm{p}_{SW}^{(r)}|$ and $|\mathrm{p}_{SSW}^{(r)}|$ measured at t_3. From the numerical simulations, we measured that the magnitude of the momentum at t_2 is not equal to that at t_1; we, therefore, denoted the magnitude of the momentum carried by the bundle at t_2 in Fig. 5(b) by $|\mathrm{p}_{SW}^{(i)}| + \Delta\mathrm{p}$. By equating the momentum of the incident SW and an unknown quantity, we can attempt to write $|\mathrm{p}_{SW}^{(i)}| + \Delta\mathrm{p}$ to $|\mathrm{p}_{SW}^{(r)}| + |\mathrm{p}_{SSW}^{(r)}|$ to obtain the equation for momentum conservation. We observe here that the difference in the magnitude of the momentum between t_1 and t_2 is not a surprise based on our demonstration in Sec. II that the velocity vs time behaviors after collision is not simply the reverse of the same before collision in the Hertz system.

We then have

$$\mathrm{E}_{SW}^{(r)}/\mathrm{E}_{SW}^{(i)} + \mathrm{E}_{SSW}^{(r)}/\mathrm{E}_{SW}^{(i)} = 1, \tag{10a}$$

$$|\mathrm{p}_{SW}^{(r)}|/|\mathrm{p}_{SW}^{(i)}| + |\mathrm{p}_{SSW}^{(r)}|/|\mathrm{p}_{SW}^{(i)}| - |\Delta\mathrm{p}|/|\mathrm{p}_{SW}^{(i)}| = 1. \tag{10b}$$

Note that the energy of the SW is related to the momentum of the SW by Eq. (9); i.e., once we are able to calculate $\Delta\mathrm{p}$ from the numerical simulations, we are able to accurately infer how much energy is devoted to generate the SSWs. We numerically measured $\Delta\mathrm{p}$ for various incident SWs [denoted with superscript (i)] with different values of p, a log–log plot of $\Delta\mathrm{p}$ as a function of p is given in Fig. 6, and the relation between $\Delta\mathrm{p}$ and $\mathrm{p}_{SW}^{(i)}$ is given as

$$|\Delta\mathrm{p}/\mathrm{p}_{SW}^{(i)}| = 0.002\,107\,85. \tag{11}$$

The results we obtain using Eqs. (9) and (10) along with knowledge of $\Delta\mathrm{p}$ from the dynamical simulations [Eq. (11)] allows the determination of $E_{SSW,phenom}$. These values are given in Table I. Our calculations stack up well when compared with directly calculated $E_{SSW,dyn}$. If we assume the simulation based numbers to be the most accurate ones, the calculated value is within 2.36% of the simulated value.

V. FINDING SSW ENERGY USING THE ANALYTIC SOLUTION OF SEN AND MANCIU AS AN INITIAL CONDITION

As proposed previously,[34] the SW in the Hertz chain can be well described by an approximate solution proposed by Sen and Manciu. This solution has the form

$$u(\alpha) = \frac{A}{2}\left\{1 - \tanh\left[\frac{f_n(\alpha)}{2}\right]\right\}, \quad f_n(z) = \sum_{q=0}^{\infty} C_{2q+1} z^{2q+1}, \tag{12}$$

with $C_1 = 2.395\,36$, $C_3 = 0.268\,529$, and $C_5 = 0.006\,134\,7$.

We first perturbed the chain with equal velocity impulses $v = 3.1129$ in opposing directions at the two ends, and then, we initiated the dynamics in the chain by starting two SWs, each satisfying Eq. (12) from the two ends. The equations of motion were integrated forward in time with these two initial conditions in both the cases. The results are shown in Fig. 7. The second and third columns in Table I show the comparisons between the predictions of our phenomenological model and dynamical simulations. It is clear that the analytical solution contains the needed features to reproduce the SSWs seen in the actual simulations.

The results from our numerical calculations, the phenomenological approach above and those using the analytic solution are captured in Table I.

VI. CONCLUSIONS

In this paper, we have presented the dynamics associated with the head-on collision of two identical and opposite propagating SWs in one dimension. We considered two systems with distinctive interaction laws between particles to carry out a comparative study. These are the integrable Toda lattice, which is a mass-spring system, and the non-integrable Hertz chain, which is a system of elastic spheres that gently touch one another. The key results reported here are summarized below.

In the Toda chain, the kinetic energy of the system goes to zero and all the energy becomes potential energy at a unique point in time, and this is when the two equal and opposite propagating SWs collide. We found that in any half of the system, the dynamics before the collision and that after collision are identical, except for being reversed in the direction of propagation.

In the Hertz system, on the other hand, the kinetic energy of the system *does not* go to zero at the point of collision but becomes very small. The central grain of the system, however, carries no kinetic energy at any time. However, the adjacent grains carry kinetic energy and do not come to a complete stop when the SWs collide. Perhaps, not surprisingly, given how different these two systems are physically, we find that the dynamics before and after the collision of the SWs is different between them. Initially, we have SWs coming toward each other. After the collision, we have SWs that carry slightly less energy followed by the SSWs that form in time after the collision. The key reason why the SSWs form is because the solitary waves cannot turn around as a unit unlike for the Toda chain.[7]

We show that using energy and momentum conservation along with the relationship connecting the energy and the momentum in a SW in a Hertz chain, shown in Eq. (9), which was deduced from the dynamical calculations, it is possible to approximately calculate the total energy in the SSWs. Since most of the energy is typically carried by the leading SSW, the energy of the SSWs obtained via this phenomenological approach is within 2.36% of the energy of the SSWs as obtained from the dynamical simulations.

Last, the solution proposed in Eq. (12) to describe the SW in a Hertz chain turns out to be useful to accurately obtain the energy carried by SSWs. We used the solitary wave solution to the equation of motion in the Hertz system[34] to time iterate the two equal and opposite propagating SWs and having them collide in the center grain of the chain. Our calculations show that the solution predicts the energy of the SSW. The error when compared to the dynamical simulations is 2.00%. The error presumably arises because the solution is not exact.

ACKNOWLEDGMENTS

S.S. acknowledges support of the Fulbright–Nehru Fellowship during the course of this work. This work was also partially supported by the National Science Foundation (NSF) under Grant Nos. DMS-1614623 and DMS-1615524.

REFERENCES

[1] M. J. Ablowitz and H. Segur, *Solitons and the Inverse Scattering Transform* (SIAM, Philadelphia, 1981).
[2] N. J. Zabusky and M. D. Kruskal, "Interaction of solitons in a collisionless plasma and the recurrence of initial states," Phys. Rev. Lett. **15**, 240–243 (1965).
[3] F. Santibanez, R. Munoz, A. Caussarieu, S. Job, and F. Melo, "Experimental evidence of solitary wave interaction in Hertzian chains," Phys. Rev. E **84**, 026604 (2011).
[4] E. Fermi, J. Pasta, and S. Ulam, "Studies of the nonlinear problems," in *Collected Papers*, edited by E. Segre (U. Chicago Press, 1965), Vol. 2, pp. 977–988.
[5] N. Flytzanis, S. Pnevmatikos, and M. Peyrard, "Discrete lattice solitons: Properties and stability," J. Phys. A: Math. Gen. **22**, 783–801 (1989).
[6] H. Zhao, Z. Wen, Y. Zhang, and D. Zheng, "Dynamics of solitary wave scattering in the Fermi-Pasta-Ulam model," Phys. Rev. Lett. **94**, 025507 (2005).
[7] M. Toda, *Theory of Nonlinear Lattices*, Springer Series in Solid-State Sciences Vol. 20 (Springer-Verlag, 1981).
[8] M. Toda, "Wave propagation in anharmonic lattices," J. Phys. Soc. Jpn. **23**, 501–506 (1967).
[9] M. Toda, "Waves in nonlinear lattice," Prog. Theor. Phys. Suppl. **45**, 174–200 (1970).
[10] M. Toda and M. Wadati, "A soliton and two solitons in an exponential lattice and related equations," J. Phys. Soc. Jpn. **34**, 18–25 (1973).
[11] H. Flaschka, "The Toda lattice: II. Existence of integrals," Phys. Rev. B **9**, 1924–1925 (1974).
[12] H. Flaschka, "On the Toda lattice: II. Inverse-scattering solution," Prog. Theor. Phys. **51**, 703–716 (1974).
[13] M. Henon, "Integrals of the Toda lattice," Phys. Rev. B **9**, 1921–1923 (1974).
[14] S. Venakides, P. Deift, and R. Oba, "The Toda shock problem," Commun. Pur. Appl. Math. **44**, 1171–1242 (1991).
[15] V. F. Nesterenko, *Dynamics of Heterogeneous Materials* (Springer-Verlag, 2001).
[16] V. F. Nesterenko, "Propagation of nonlinear compression pulses in granular media," J. Appl. Mech. Tech. Phys. **24**(5), 733–743 (1983).
[17] V. F. Nesterenko, A. N. Lazaridi, and E. B. Sibiryakov, "The decay of soliton at the contact of two 'acoustic vacuums'," J. Appl. Mech. Tech. Phys. **36**, 166–168 (1995).
[18] R. S. Sinkovits and S. Sen, "Nonlinear dynamics in granular columns," Phys. Rev. Lett. **74**, 2686–2689 (1995).
[19] S. Sen and R. S. Sinkovits, "Sound propagation in impure granular columns," Phys. Rev. E **54**, 6857–6865 (1996).
[20] C. Coste, E. Falcon, and S. Fauve, "Solitary waves in a chain of beads under Hertz contact," Phys. Rev. E **56**, 6104–6117 (1997).
[21] H. Hertz, "Über die berührung fester elastischer Körper (On the contact of rigid elastic solids)," J. Reine Angew. Math. **92**, 156–171 (1881).
[22] M. Manciu, S. Sen, and A. J. Hurd, "Crossing of identical solitary waves in a chain of elastic beads," Phys. Rev. E **57**, 016614 (2000).
[23] F. S. Manciu and S. Sen, "Secondary solitary wave formation in systems with generalized Hertz interactions," Phys. Rev. E **66**, 016616 (2002).
[24] E. Ávalos and S. Sen, "How solitary waves collide in discrete granular alignments," Phys. Rev. E **79**, 046607 (2009).
[25] S. Job, F. Melo, A. Sokolow, and S. Sen, "How Hertzian solitary waves interact with boundaries in a 1D granular medium," Phys. Rev. Lett. **94**, 178002 (2005).
[26] M. Przedborski, T. A. Harroun, and S. Sen, "Granular chains with soft boundaries: Slowing the transition to quasi-equilibrium," Phys. Rev. E **91**, 042207 (2015).
[27] S. Sen, T. R. K. Mohan, and J. M. M. Pfannes, "The quasi-equilibrium phase in nonlinear 1D systems," Physica A **342**, 336 (2004).
[28] E. Ávalos, D. Sun, R. L. Doney, and S. Sen, "Sustained strong fluctuations in a nonlinear chain at acoustic vacuum: Beyond equilibrium," Phys. Rev. E **84**, 046610 (2011).
[29] E. Ávalos and S. Sen, "Granular chain between asymmetric boundaries and the quasiequilibrium state," Phys. Rev. E **89**, 053202 (2014).
[30] S. Sen, J. Hong, J. Bang, E. Ávalos, and R. Doney, "Solitary waves in the granular chain," Phys. Rep. **2**, 21–66 (2008).
[31] M. Przedborski, S. Sen, and T. A. Harroun, "The equilibrium phase in heterogeneous Hertzian chains," J. Stat. Mech. **2017**, 123204.
[32] B. Neyenhuis, J. Zhang, P. W. Hess, J. Smith, A. C. Lee, P. Richerme, Z. X. Gong, A. V. Gorshkov, and C. Monroe, "Observation of prethermalization in long-range interacting spin chains," Sci. Adv. **3**(8), e1700672 (2017).
[33] A. W. Barnard, M. Zhang, G. S. Wiederhecker, M. Lipson, and P. L. McEuen, "Real-time vibrations of a carbon nanotube," Nature **566**(7742), 89 (2019).
[34] S. Sen and M. Manciu, "Solitary wave dynamics in generalized Hertz chains: An improved solution of the equation of motion," Phys. Rev. E **64**, 056605 (2001).
[35] M. A. Hasan and S. Nemat-Nasser, "Basic properties of solitary waves in granular crystals," J. Mech. Phys. Solids **101**, 1 (2017).
[36] M. P. Allen and D. J. Tildesley, *Computer Simulation of Liquids* (Clarendon Press, Oxford, 1987).
[37] A. M. Tichler, L. R. Gómez, N. Upadhyaya, X. Campman, V. F. Nesterenko, and V. Vitelli, "Transmission and reflection of strongly nonlinear solitary waves at granular interfaces," Phys. Rev. Lett. **111**, 048001 (2013).